

Effect of anisotropic strain on the charge ordering behavior in $\text{Bi}_{0.4}\text{Ca}_{0.6}\text{MnO}_3$ films

Y. H. Ding, Y. Q. Wang, R. S. Cai, Y. Z. Chen, and J. R. Sun

Citation: *Appl. Phys. Lett.* **99**, 191914 (2011); doi: 10.1063/1.3660722

View online: <http://dx.doi.org/10.1063/1.3660722>

View Table of Contents: <http://apl.aip.org/resource/1/APPLAB/v99/i19>

Published by the [American Institute of Physics](#).

Related Articles

On the theoretical description of nucleation in confined space
AIP Advances **1**, 042160 (2011)

Threading-dislocation blocking by stacking faults formed in an undoped GaN layer on a patterned sapphire substrate
Appl. Phys. Lett. **99**, 211901 (2011)

Negative ions: The overlooked species in thin film growth by pulsed laser deposition
Appl. Phys. Lett. **99**, 191501 (2011)

Atomistic surface erosion and thin film growth modelled over realistic time scales
J. Chem. Phys. **135**, 174706 (2011)

Growth of Ruddlesden-Popper type faults in Sr-excess SrTiO_3 homoepitaxial thin films by pulsed laser deposition
Appl. Phys. Lett. **99**, 173109 (2011)

Additional information on *Appl. Phys. Lett.*

Journal Homepage: <http://apl.aip.org/>

Journal Information: http://apl.aip.org/about/about_the_journal

Top downloads: http://apl.aip.org/features/most_downloaded

Information for Authors: <http://apl.aip.org/authors>

ADVERTISEMENT

**AIPAdvances**

Submit Now

**Explore AIP's new
open-access journal**

- **Article-level metrics
now available**
- **Join the conversation!
Rate & comment on articles**

Effect of anisotropic strain on the charge ordering behavior in $\text{Bi}_{0.4}\text{Ca}_{0.6}\text{MnO}_3$ films

Y. H. Ding,¹ Y. Q. Wang,^{1,a)} R. S. Cai,¹ Y. Z. Chen,² and J. R. Sun²

¹The Cultivation Base for State Key Laboratory, Qingdao University, No. 308 Ningxia Road, Qingdao 266071, People's Republic of China

²State Key Laboratory of Magnetism and Beijing National Laboratory for Condensed Matter Physics, Institute of Physics, Chinese Academy of Sciences, Beijing 100080, People's Republic of China

(Received 23 August 2011; accepted 26 October 2011; published online 11 November 2011)

Anisotropic strain has a significant influence on the charge ordering (CO) behavior in $\text{Bi}_{0.4}\text{Ca}_{0.6}\text{MnO}_3$ (BCMO) films on (110) SrTiO_3 substrates. Effect of film thickness on the CO behavior in BCMO films was investigated at 103 K using transmission electron microscopy. It was found that the film has undergone a structural transformation with the increase of film thickness, i.e., from no modulation to a localized incommensurate modulation and further to a commensurate modulation. The distinctive thickness-dependent CO transition has a close relationship with the anisotropic strain relaxation process. Structural models are proposed to explain the modulated structures in the films. © 2011 American Institute of Physics. [doi:10.1063/1.3660722]

The perovskite manganites have attracted a lot of interest for their colossal magnetoresistance (CMR) effect. Apart from the CMR effect, the manganites also exhibit intriguing physical properties such as insulator-metal¹ and/or structural transition² induced by applied magnetic-field or photon radiation, phase separation,³ charge/orbital ordering (CO/OO),⁴ cluster-spin glass transition,⁵ etc. The CO/OO is one of the most important physical properties associated with the strong spin-lattice-charge coupling.

Bismuth-based manganites are attractive because of their CO/OO transition temperature, which can be well above the room temperature in some cases.⁶ For bulk manganites, anisotropy is usually not obvious due to the high structural symmetry. In contrast, thin films exhibit lattice strains that can strongly affect their physical properties.^{7,8} Thus, it is important to investigate the strain effect on the CO behaviors in the films.^{9–11} A lot of research has focused on the investigation of physical properties for $\text{Bi}_{0.4}\text{Ca}_{0.6}\text{MnO}_3$ (BCMO) films. Chen *et al.*^{12–14} systematically studied the effect of strain on the CO transition and the electronic transport properties of BCMO films. In this paper, we report transmission electron microscopy (TEM) studies of the strain effect on CO behaviors in BCMO epitaxial films grown on a (110) SrTiO_3 (STO) substrate. All the TEM studies were carried out at 103 K. Selected area electron diffraction (SAED) technique and high-resolution transmission electron microscopy (HRTEM) imaging are employed to investigate the CO behaviors in the BCMO epitaxial films.

Epitaxial BCMO films were prepared on a (110) STO substrate by pulsed laser deposition (PLD) technique (laser wavelength = 248 nm, repetition rate = 5 Hz, and fluency = 7 J/cm^2) from a target with a nominal composition of BCMO. During the deposition, the substrate temperature was kept at $\sim 700^\circ\text{C}$ and the oxygen pressure at $\sim 60\text{ Pa}$. The film thickness is 10, 40, 110, and 200 nm, controlled by deposition time. Structural analyses of the films were performed by

x-ray diffraction (XRD) analysis on a Philips X'pert Pro diffractometer using $\text{Cu K}\alpha_1$ radiation. The specimens for TEM examinations were prepared in a cross-sectional orientation ($[\bar{1}11]$ and $[1\bar{1}0]$ zone-axes for the STO substrates) using conventional techniques of mechanical polishing and ion thinning. The ion milling was performed using a Gatan Model 691 Precision Ion Polishing System (PIPS). A JEOL JEM 2100F transmission electron microscope with a low-temperature sample stage was used for bright field (BF), SAED, and HRTEM imaging. The temperature was set and maintained by a Gatan SmartSet cold stage controller (636.MA). All the TEM studies were carried out at 103 K, close to a liquid nitrogen temperature.

No modulation structure has been observed for the BCMO films thinner than 100 nm. Figure 1(a) shows a $[\bar{1}11]$ zone-axis HRTEM image of BCMO film with a thickness of 40 nm taken at 103 K, where the interface between STO and BCMO is indicated by two arrows. It can be seen that the HRTEM image is flat and no evident stripes can be observed. The HRTEM result is consistent with the conclusion drawn from our SAED pattern. Figure 1(b) is the diffraction pattern taken from the BCMO film in Fig. 1(a) at 103 K, and no superlattice spots are observed, which is similar to the SAED pattern obtained at room temperature.¹⁵ Therefore, it is clear that there is no difference in the SAED patterns recorded at low temperature (103 K) and room temperature for the film

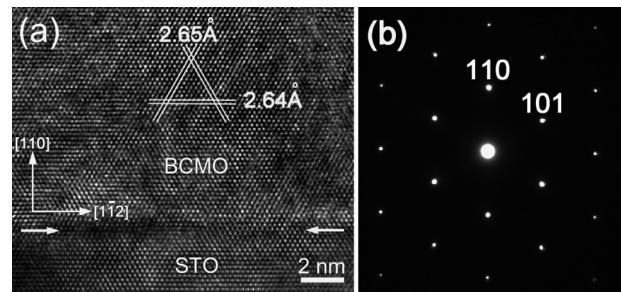


FIG. 1. HRTEM images and SAED patterns taken from thinner films at 103 K, (a) and (b) film thickness is 40 nm.

^{a)} Author to whom correspondence should be addressed. Electronic mail: yqwang@qdu.edu.cn.

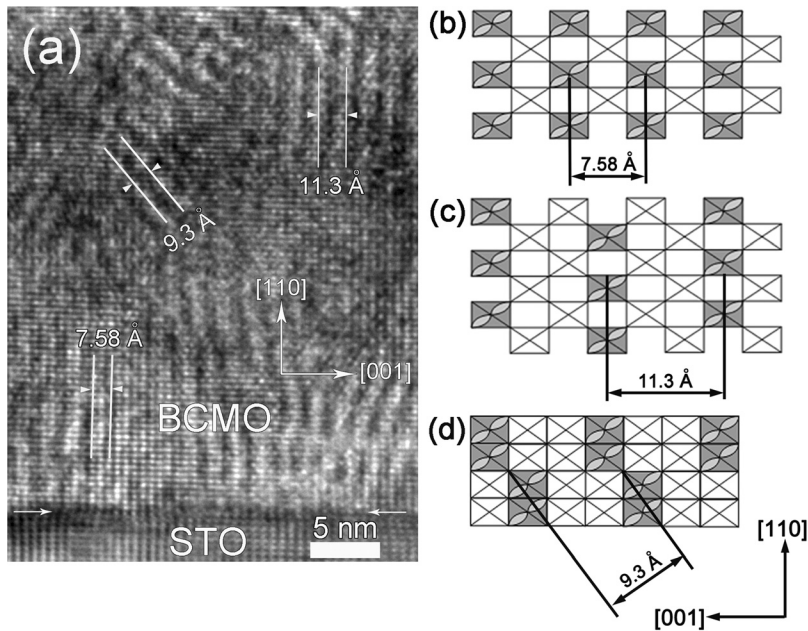




FIG. 2. (a) HRTEM image of BCMO/STO interface region with a film thickness of 110 nm. (b)–(d) Schematic models for the CO behaviors in the BCMO film.  and  represent Mn³⁺ and Mn⁴⁺, respectively.

with a thickness less than 100 nm. This indicates that CO is absent in the films with a thickness less than 100 nm.

When the film thickness increases to 110 nm, modulation structure appears. Figure 2(a) shows the $[1\bar{1}0]$ zone-axis HRTEM image of the film of 110 nm, recorded at 103 K. The interface between BCMO and STO is indicated by two arrows. Stripes can be clearly seen from Fig. 2(a), and the stripe direction varies from location to location, rather than being uniform. Extensive HRTEM investigation showed that the modulated stripes were formed along the directions of $[001]$ and $[112]$. It can be seen that near the interface region the modulated stripes are along the $[001]$ direction and its periodicity is about 7.58 Å. Modulations with a periodicity of 11.3 Å are also observed in the $[001]$ direction. In the regions a little far away from the BCMO/STO interface, the film has fringes with different directions. One of the modulation directions can be determined to be $[112]$, and the fringe periodicity is measured to be about 9.3 Å. Figure 2(a) shows several kinds of modulated structures in the 110-nm-thick

film (details about the other modulated structures will be reported elsewhere). Based on the HRTEM observations, structural models (after Wang *et al.*¹⁶) for CO phases in the film of 110 nm can be obtained, schematically shown in Figs. 2(b)–2(d). Three different types of modulation models are shown, along the $[001]$ and $[112]$ directions, respectively. Figure 2(b) is one of the model for the modulated structure along the $[001]$ direction, and its periodicity is about 7.58 Å. Figure 2(c) is one of the other model for the modulated structure along the $[001]$ direction with a periodicity of 11.3 Å. Figure 2(d) is the model for the modulated structure along the $[112]$ direction with a periodicity of 9.3 Å. The Mn³⁺ and Mn⁴⁺ ions in the film are arranged in order due to the strain effects.

Figure 3(a) shows a $[1\bar{1}0]$ zone-axis HRTEM image of the film with a thickness of 200 nm, recorded at 103 K. The modulation is found to be uniform, with the direction along the $[111]$ direction and the lattice spacing (4.4 Å) is doubled compared with that at the room temperature. This suggests

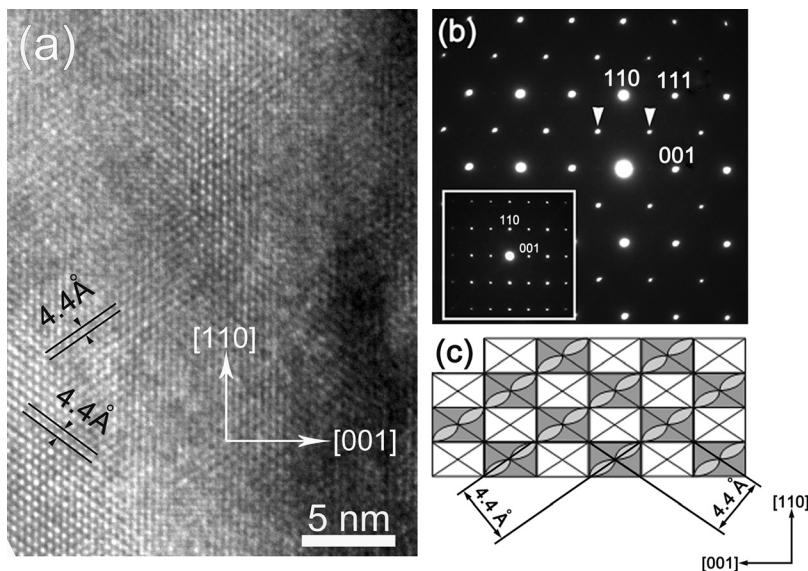




FIG. 3. (a) HRTEM image of BCMO film with a thickness of 200 nm at 103 K. (b) SAED pattern taken from the BCMO film in (a) at 103 K. Inset shows a typical SAED pattern taken at the room temperature. (c) Schematic model for the CO behavior in the BCMO film.  and  represent Mn³⁺ and Mn⁴⁺, respectively.

the appearance of superstructure, which is confirmed by the SAED result. Figure 3(b) is a $[1\bar{1}0]$ zone-axis diffraction pattern recorded at 103 K. Superlattice spots along $\{111\}$ directions can be identified, which is obviously different from results obtained at room temperature (inset in Fig. 3(b)). These superlattice spots are caused by the CO of Mn^{3+} and Mn^{4+} in the BCMO film. The modulated structure is characterized as a commensurate modulation, where the superlattice spots locate at the half position between transmitted spot and $\{111\}$ diffracted spots. The modulation periodicity is about 4.4 Å, which is twice the spacing between (111) planes. Based on the SAED and HRTEM observations, structural model (after Wang *et al.*¹⁶) for CO behavior in the films with the thickness of 200 nm is demonstrated in Fig. 3(c). From Fig. 3(c), it can be seen that the modulation structure is commensurate and the Mn^{3+} and Mn^{4+} are in good order along the $[111]$ direction. Thus, the modulation periodicity is doubled, compared with the structure at room temperature.

Generally speaking, the CO state has a close relationship with the strain, which depends on the film thickness. HRTEM images demonstrate that with the increase of film thickness, the lattice spacing along the direction parallel to the BCMO/STO interface decreases because the interplanar spacings for both (101) and $(01\bar{1})$ planes are reduced, while the spacing along the direction perpendicular to the BCMO/STO interface increases. For the 10-nm-thick BCMO film, it was fully relaxed along the $[1\bar{1}2]$ direction, but it had a partial relief along the direction parallel to the BCMO/STO interface. HRTEM image at low temperature is not different to that at room temperature. For 40-nm-thick film, the lattice spacing along the $[1\bar{1}2]$ direction is smaller than that in the 10-nm-thick film, while the lattice spacing along the $[110]$ direction is bigger than that in the 10-nm-thick film. This indicates that the compressive strain in the parallel direction makes lattice spacing smaller and the tensile strain in the perpendicular direction makes the lattice spacing bigger. The lattice strain along the $[1\bar{1}2]$ direction will remain until the thickness exceeds 100 nm. As a consequence, no clear CO can be observed for films thinner than 100 nm. When the thickness reaches 110 nm, the lattice spacing along the $[110]$ direction is bigger than that in 40-nm-thick film. This suggests that the residual strain along the $[1\bar{1}2]$ and $[110]$ directions decreases as the thickness increases. The strain along the two directions is different, so the strain in the BCMO film with the thickness of 110 nm is anisotropic. At room temperature, no modulated structure can be observed in the HRTEM images. However, when the temperature is reduced to 103 K, evident modulated stripes can be observed in the HRTEM image of the 110-nm-thick film. When the thickness reaches 200 nm, the strain in the film can be released by the formation of dislocations. The strain state of the film is similar to that in the bulk materials, and only one type of modulation along the $[111]$ direction has been found. Our

TEM result is consistent with the previous report¹² on the CO transition degree as a function of film thickness. Therefore, the CO at low temperature is dependent on the strain states in the BCMO films.

In conclusion, the effects of strain on CO in the BCMO films with thicknesses of 10, 40, 110, and 200 nm were studied at 103 K using SAED and HRTEM. The present study indicated that with the increase of the BCMO film thickness, the films have undergone structural transformations, i.e., from no modulation to a localized incommensurate modulation, and further to a commensurate modulation. Structural models, based on the HRTEM observation, were proposed for the modulated structures in the BCMO films with thicknesses of 110 and 200 nm.

The authors would like to thank the financial support from the National Natural Science Foundation of China (Grant Nos. 10974105 and 50832007), National Basic Research of China (Grant Nos. 2007CB925002 and 2011CB921801), the Natural Science Foundation for Outstanding Young Scientists in Shandong Province (Grant No. JQ201002), the Project of Introducing Talents to Support Thousand Talents Programs (Grant No. P201101032), the Program of Science and Technology in Qingdao City (Grant No. 11-2-4-23-hz), and the Scientific Research Starting Foundation for the Introduced Talents at Qingdao University (Grant No. 06300701). Y.Q. Wang would also like to thank the financial support from Taishan Overseas Scholar Program of Shandong Province.

¹J. Q. He, V. V. Volkov, T. Asaka, S. Chaudhuri, R. C. Budhani, and Y. Zhu, *Phys. Rev. B* **82**, 224404 (2010).

²J. Q. He, V. V. Volkov, M. Beleggia, T. Asaka, J. Tao, M. A. Schofield, and Y. Zhu, *Phys. Rev. B* **81**, 094427 (2010).

³M. M. Savosta and P. Novák, *Phys. Rev. Lett.* **87**, 137204 (2001).

⁴Y. D. Chuang, A. D. Gromko, D. S. Dessau, T. Kimura, and Y. Tokura, *Science* **292**, 1509 (2001).

⁵C. Autret, A. Maignan, C. Martin, M. Hervieu, V. Hardy, S. Hébert, and B. Raveau, *Appl. Phys. Lett.* **82**, 4746 (2003).

⁶H. Woo, T. A. Tyson, M. Croft, S. W. Cheong, and J. C. Woicik, *Phys. Rev. B* **63**, 134412 (2001).

⁷A. J. Millis, *Nature* **392**, 147 (1998).

⁸W. Prellier, P. Lecoeur, and B. Mercey, *J. Phys.: Condens. Matter* **13**, R915 (2001).

⁹Y. Wakabayashi, D. Bizen, H. Nakao, Y. Murakami, M. Nakamura, Y. Ogimoto, K. Miyano, and H. Sawa, *Phys. Rev. Lett.* **96**, 017202 (2006).

¹⁰M. Nakamura, Y. Ogimoto, H. Tamaru, M. Izumi, and K. Miyano, *Appl. Phys. Lett.* **86**, 182504 (2005).

¹¹D. H. Kim, H. M. Christen, M. Varela, H. N. Lee, and D. H. Lowndes, *Appl. Phys. Lett.* **88**, 202503 (2006).

¹²Y. Z. Chen, J. R. Sun, S. Liang, W. M. Lv, B. G. Shen, and W. B. Wu, *J. Appl. Phys.* **103**, 096105 (2008).

¹³Y. Z. Chen, J. R. Sun, D. J. Wang, S. Liang, J. Z. Wang, Y. N. Han, B. S. Han, and B. G. Shen, *J. Phys.: Condens. Matter* **19**, 442001 (2007).

¹⁴Y. Z. Chen, J. R. Sun, S. Liang, W. M. Lu, and B. G. Shen, *J. Appl. Phys.* **104**, 113913 (2008).

¹⁵Y. H. Ding, R. S. Cai, Q. T. Du, Y. Q. Wang, Y. Z. Chen, and J. R. Sun, *J. Cryst. Growth* **317**, 115 (2011).

¹⁶Y. Q. Wang, X. F. Duan, Z. H. Wang, and B. G. Shen, *Appl. Phys. Lett.* **78**, 2157 (2001).